

Discovery of Inhibitors of *Trypanosoma brucei* by Phenotypic Screening of a Focused Protein Kinase Library

Andrew Woodland,^[a] Stephen Thompson,^[a] Laura A. T. Cleghorn,^[a] Neil Norcross,^[a] Manu De Rycker,^[a] Raffaella Grimaldi,^[a] Irene Hallyburton,^[a] Bhavya Rao,^[a] Suzanne Norval,^[a] Laste Stojanovski,^[a] Reto Brun,^[b] Marcel Kaiser,^[b] Julie A. Frearson,^[a] David W. Gray,^[a] Paul G. Wyatt,^[a] Kevin D. Read,^[a] and Ian H. Gilbert^{*[a]}

A screen of a focused kinase inhibitor library against *Trypanosoma brucei rhodesiense* led to the identification of seven series, totaling 121 compounds, which showed >50% inhibition at 5 μM . Screening of these hits in a *T. b. brucei* proliferation assay highlighted three compounds with a 1*H*-imidazo[4,5-*b*]pyrazin-2(3*H*)-one scaffold that showed sub-micromolar activity and excellent selectivity against the MRC5 cell line. Subsequent rounds of optimisation led to the identification of compounds that exhibited good in vitro drug metabolism and pharmacokinetics (DMPK) properties, although in general this

series suffered from poor solubility. A scaffold-hopping exercise led to the identification of a 1*H*-pyrazolo[3,4-*b*]pyridine scaffold, which retained potency. A number of examples were assessed in a *T. b. brucei* growth assay, which could differentiate static and cidal action. Compounds from the 1*H*-imidazo[4,5-*b*]pyrazin-2(3*H*)-one series were found to be either static or growth-slowing and not cidal. Compounds with the 1*H*-pyrazolo[3,4-*b*]pyridine scaffold were found to be cidal and showed an unusual biphasic nature in this assay, suggesting they act by at least two mechanisms.

Introduction

Human African trypanosomiasis (HAT), or sleeping sickness, as it is more commonly known, is an often fatal infection endemic in sub-Saharan Africa. Current treatments for HAT are inadequate due to toxicity and inappropriate means of administration for remote rural settings, where the disease is predominantly found. Fortunately, the number of cases of HAT appears to be decreasing; however, there is an urgent need for new effective treatments for HAT, to improve treatment and to facilitate the eventual eradication of this disease. HAT is caused by the protozoan parasites *Trypanosoma brucei gambiense* and *T. b. rhodesiense*. The parasites have a complex life cycle, involving the human host and the tsetse fly, which is the vector. Initially there is a peripheral infection in which the parasite is pre-

dominantly found in the blood. However, the parasites eventually invade the central nervous system, which can lead to coma and death.^[1,2]

Protein kinases are a major drug target for human diseases, particularly oncology.^[3] Analysis of the *T. brucei* genome indicates that there are 156 protein kinases in the trypanosome kinome.^[4-6] Whilst parasite protein kinases have been relatively poorly investigated, there appear to be significant differences from human kinases. In particular:

- A relatively large number of protein kinases associated with cell-cycle control, which may be a consequence of the complex life cycle of the parasite;
- A lack of tyrosine kinases (except dual-specificity kinases);
- A number of unique kinases.

In addition, a number of protein kinases have been genetically validated as potential drug targets in *T. brucei* using RNA interference (RNAi) or gene knockouts.^[4,5,7-9] Given that protein kinases are generally known to be druggable, they represent promising drug targets in trypanosomatids. The Drug Discovery Unit (DDU) in Dundee has recently carried out screens and chemical optimisation programmes against several parasite protein kinases. Although we have prepared compounds with significant (low-nanomolar) activity against the proteins, this did not always translate into potent cellular activity.^[10]

A complementary method to target-based drug discovery is phenotypic drug discovery,^[11] which has several advantages. Firstly, all possible drug discovery targets are present in their natural environment, allowing an unbiased and more physio-

[a] Dr. A. Woodland,⁺ Dr. S. Thompson,⁺ Dr. L. A. T. Cleghorn, Dr. N. Norcross, Dr. M. De Rycker, Dr. R. Grimaldi, I. Hallyburton, Dr. B. Rao, S. Norval, L. Stojanovski, Prof. J. A. Frearson, Dr. D. W. Gray, Prof. P. G. Wyatt, Dr. K. D. Read, Prof. I. H. Gilbert
Drug Discovery Unit, Division of Biological Chemistry and Drug Discovery
University of Dundee, Dundee, DD1 5EH (UK)
E-mail: i.h.gilbert@dundee.ac.uk

[b] Prof. R. Brun, Dr. M. Kaiser
Swiss Tropical and Public Health Institute
Socinstrasse 57, P.O. Box, 4002 Basel (Switzerland)

[*] These authors contributed equally to this work.

Supporting information for this article is available on the WWW under <http://dx.doi.org/10.1002/cmdc.201500300>: synthesis details for all compounds and additional biological data.

© 2015 The Authors. Published by Wiley-VCH Verlag GmbH & Co. KGaA. This is an open access article under the terms of the Creative Commons Attribution License, which permits use, distribution and reproduction in any medium, provided the original work is properly cited.

logically relevant screening platform; this may give rise to compounds that inhibit more than one target. Indeed it has been found in the oncology field that compounds that inhibit more than one protein kinase are often required for activity. Secondly, as the primary screening platform is a functional efficacy screen, the relationship between target and phenotype does not need to be established. Finally, compounds must be able to penetrate cells and have a sufficient free fraction in the assay to elicit their response, eliminating compounds with inappropriate properties.^[12–14] We therefore decided to conduct a phenotypic screen of a focused kinase compound library against whole parasites. A similar exercise was recently reported by Diaz et al., in which a phenotypic screen of a kinase-targeted library from GlaxoSmithKline (GSK) was reported and gave rise to a number of actives.^[15] There is also a recent report of a large screen against kinetoplastids with 1.8 million compounds from GSK.^[16] The ideal target product profile to treat HAT requires a compound that can treat both stage 1 (peripheral) and stage 2 (CNS) infection;^[6] thus the compound should have blood–brain barrier (BBB) permeability.

Results and Discussion

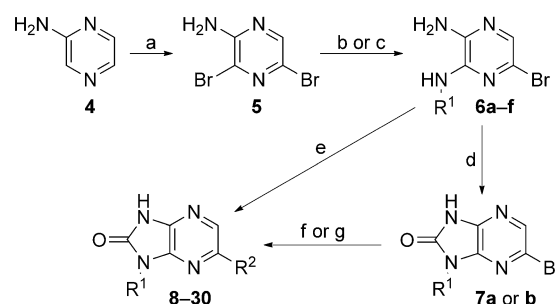
The focused screen

The Dundee focused protein kinase library,^[17] which at that point contained 3885 compounds, was assayed by the Swiss Tropical and Public Health Institute (STPH) against *T. b. rhodesiense* at 1 and 5 μM . From this original triage, seven series, totaling 121 compounds, were identified which showed >50% inhibition of parasite growth at 5 μM . These were progressed into EC₅₀ determination in a *T. b. brucei* proliferation assay and assessed in a MRC5 proliferation assay to provide an early indicator of toxicity to mammalian cells. From this, seven compounds showed EC₅₀ values <1 μM against *T. b. brucei*. The most active hit compound was a 1*H*-imidazo[4,5-*b*]pyrazin-2(3*H*)-one (**1**), which had an EC₅₀ value of 80 nM against *T. b. brucei* and was nontoxic to the mammalian MRC5 cell line (EC₅₀ >50 μM). Two additional 1*H*-imidazopyrazinone analogues had EC₅₀ values of <1 μM against *T. b. brucei* (Table 1).

The physicochemical properties were calculated in StarDrop (www.optibrium.com). It has been proposed that for a compound to have BBB permeability, it should have a topological polar surface area (tPSA) of <90 Å² and a molecular weight (*M_r*) less than 450 Da.^[18] Wager's research group have proposed more sophisticated models.^[19–21] The *M_r* and tPSA values were all within the preferred range for a potential CNS-penetrant compound. The calculated log*P* values were also in the range of CNS-penetrant compounds.^[19] Based on the initial data we decided to progress the project into hits-to-leads development.

Hit validation

Medicinal chemistry was initiated with the aim of validating and profiling the hit series and increasing the potency of the compounds. The desired 1*H*-imidazopyrazinones were synthesised in four steps from 2-aminopyrazine **4**. Bromination with NBS gave the versatile scaffold 2,5-dibromo-4-aminopyrazine **5**. Regioselective displacement of the 5-bromine group with amines could be conducted using microwave heating to give intermediates **6a–f** (Scheme 1). Compounds **8–11**, **13–15**, **17**,



Scheme 1. Reagents and conditions: a) NBS, MeCN, 18 h, RT, 12%; b) amine, DIPEA, EtOH, 180 °C (microwave), 30 min, 27–64%; c) cyclohexylamine, DIPEA, *n*BuOH, 220 °C (microwave), 30 min, 95%; d) CDI, 1,4-dioxane, 80 °C, 16 h, 31%; e) for **8–11**, **13–15**, **17**, and **18**: 1) Pd(PPh₃)₄ (3 mol%), K₂CO₃ (1.5 M aqueous), boronic acid, DMF, 140 °C, 5 min; 2) CDI, 1,4-dioxane, 140 °C, 20 min, 3–34%; f) for **12** and **19–30**: Pd(PPh₃)₄ (3 mol%), K₂CO₃ (1.5 M aqueous), boronic acid, DMF, 140 °C, 5 min, 7–67%; g) for **16**: **7**, H₂, 5% Pd/C, MeOH, 15%.

Table 1. Potency of hits 1–3.

ID	clog <i>P</i>	tPSA [Å ²]	<i>M_r</i> [Da]	EC ₅₀ [μM] ^[a]	
				<i>T. b. brucei</i>	MRC5
1	3.3	57	334	0.08	> 50
2	2.8	75	370	0.5	15
3	2.9	77	334	0.9	ND

[a] Values are the geometric mean of two or more determinations; standard deviation is typically within 2-fold of the EC₅₀ value. ND: not determined.

and **18** were prepared by Suzuki reaction with the appropriate diamine precursor followed by cyclisation with CDI. Cyclisation of the appropriate diamine (**6a** or **b**) with CDI gave **7a** or **7b**, which were then reacted under Suzuki conditions to give compounds **12** and **19–30**. Treatment of **7a** under hydrogenation conditions afforded compound **16**.

Enantiomers **1** and **8** were equipotent, whilst removal of the benzylic methyl group (compound **9**) resulted in a fivefold decrease in activity (Table 2). Replacement of the benzyl group with methylcyclopropane (compound **10**) had little effect on the activity, whilst further truncation of the amine to a methyl group (in **11**) resulted in a 100-fold drop in activity relative to methyl cyclopropane (in **10**). Replacement

Table 2. Variation of the R¹ group of compound 1.

ID	R ¹	R ²	clogP	EC ₅₀ [μ M] ^[a]		Aq. Sol. [μ M] ^[b]
				<i>T. b. brucei</i>	MRC5	
1			3.6	0.08	> 50	< 12
8			3.6	0.09	> 50	ND
9			3.3	0.5	> 50	ND
10			2.7	0.3	> 50	ND
11	Me		1.9	40	> 50	ND
12			3.9	0.03	> 50	55
13			2.0	0.59	> 50	ND

[a] Values are the geometric mean of two or more determinations; standard deviation is typically within 2-fold of the EC₅₀ value. [b] Aqueous kinetic solubility. ND: not determined.

of the methylbenzyl group of **1** with a methoxypropyl group (in **13**) resulted in a sevenfold loss in activity. Interestingly, replacement of the methylbenzyl group of **1** with cyclohexane (compound **12**) resulted in a threefold improvement in activity. Compounds showed good selectivity for the parasite over MRC5 cells.

The 4-fluorophenyl group of **1** could be replaced with a phenyl ring (in **14**) with no loss of activity (Table 3). The larger 4-trifluoromethoxy analogue **15** was 10-fold less active than **1**, but was comparable with the hit compound **2**, further demonstrating that changes to the R¹ group were tolerated. Replacement of the phenyl ring of **14** with a hydrogen atom in **16** resulted in a >300-fold loss of activity relative to **14**. Substitution of the phenyl ring with a 3-fluoro group was tolerated in **17**, while the larger and more polar 3-methanesulfonamide group (in **18**) resulted in a 30-fold loss of activity.

Kinase panel and DMPK data

These data validated the series, as there was a definite structure activity relationship, and several examples demonstrated sub-100 nM EC₅₀ values in the *T. b. brucei* proliferation assay. The compounds also showed excellent selectivity over human MRC5 cells. Consequently, it was decided to profile the com-

Table 3. Variation of the R² group of compound 1.

ID	R ¹	R ²	clogP	EC ₅₀ [μ M] ^[a]		Aq. Sol. [μ M] ^[b]
				<i>T. b. brucei</i>	MRC5	
1			3.6	0.08	> 50	< 12
14			3.5	0.1	26	< 12
15			4.0	1	39	ND
16		H	2.0	36	> 50	ND
17			3.6	0.3	44	ND
18			2.5	3	46	ND

[a] Values are the geometric mean of two or more determinations; standard deviation is typically within 2-fold of the EC₅₀ value. [b] Aqueous kinetic solubility. ND: not determined.

pounds further for potential inhibition of human kinases and to study their DMPK properties to ensure that there were no major issues which may impact further development.

The DDU kinase-focused compound set contains lead-like scaffolds that are designed to target protein kinases; they have kinase hinge binding motifs. Four of the 1*H*-imidazopyrazinones were screened against a human/mammalian kinase panel at the University of Dundee (www.kinase-screen.mrc.ac.uk) at a concentration of 10 μ M. At the time of testing the panel contained 79 mammalian kinases selected to provide a broad coverage of the mammalian kinome (~500 kinases in the human genome).^[3] None of the compounds were active against any of the kinases at 10 μ M. Although the results did not provide any clues as to the molecular target in the parasite, they did show the 1*H*-imidazopyrazinones to have promising selectivity over mammalian kinases.

Two key compounds, **1** and **12**, showed low in vitro mouse hepatic microsomal intrinsic clearance ($CL_{int} < 0.5$ and $0.7 \text{ mL min}^{-1} \text{ g}^{-1}$, respectively), consistent with good metabolic stability. Compound **1**, with promising in vitro anti-parasitic activity, low toxicity to human cells, and promising in vitro metabolic stability, was progressed into in vivo pharmacokinetic (PK) determination. After a single oral dose at 5 mg kg^{-1} to female NMRI mice, the compound showed a low C_{max} value and took approximately 2 h to reach C_{max} , both of which are suggestive of solubility-limited absorption (Table 4). Furthermore, **1** showed high protein binding (0.3% unbound). Conse-

Table 4. PK data for compound 1.

Route	Dose [mg kg ⁻¹]	C _{max} [ng mL ⁻¹] ^[a]	t _{max} [h] ^[b]	AUC ₍₀₋₈₎ [ng min mL ⁻¹] ^[c]	t _{1/2} [h] ^[d]
p.o.	5	110	4	36000	3

[a] Maximum concentration reached. [b] Time after initial dose at which C_{max} was reached. [c] Area under the curve. [d] Half-life of compound in the blood.

quently, the observed free blood concentration was likely to be too low for the compound to be efficacious in vivo even at high dose, so further development was required to improve free oral exposure for 1. Common strategies to address the key issues of poor solubility and/or high protein binding include decreasing the lipophilicity (log*P*), addition of solubilising groups, and reducing the planarity of the molecule to minimise crystal stacking.^[22–25]

Hit to leads

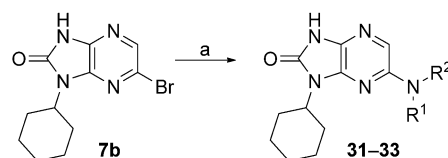
The R² position

A round of optimisation for the R² position was commenced. During this process R¹ was retained as a cyclohexyl moiety, as this substituent gave the greatest activity and, due to its non-planar structure, should also increase the solubility of the compounds. A variety of substituents were investigated at the *para*, *meta*, and *ortho* positions of the phenyl group at the R² position. The substituents were designed either to disrupt the packing and/or to reduce lipophilicity. Compounds were prepared using the route described in Scheme 1 (Table 5).

For the *para*-substituted compounds, the electron-donating methoxy group in 20 showed an eightfold drop in activity. The

introduction of polar groups was poorly tolerated, with hydroxymethyl compound 21 being 10-fold less active, while amide 22 and dimethylaminomethyl compound 23 were 30- and 50-fold less active, respectively. Substituents at the *para* position generally caused a drop in activity, relative to those in the *ortho* or *meta* positions. Encouragingly, the hydroxymethyl substituents retained activity in the *ortho* and *meta* positions (28 and 24, respectively) and gave rise to good solubility.

Further work was undertaken in which the phenyl ring of 19 was replaced with a heterocycle or saturated ring system, which should increase solubility. For the introduction of amines we used a Buchwald reaction on intermediate 7b (Scheme 2). For the introduction of aromatic heterocycles we used the chemistry described above. Both 4-pyridyl 29 and 3-pyridyl 30 compounds were equipotent to phenyl 19, demonstrating a tolerance for a hydrogen bond acceptor at the 3- and 4-positions (Table 6). Both piperidine 31 and the more polar morpholine 32 were tolerated, but the basic piperazine 33 was 50-fold less active than the phenyl compound 19.



Scheme 2. Reagents and conditions: a) Pd₂dba₃ (5 mol%), amine (2 equiv), rac-binap (10 mol%), tBuOK (3 equiv), 1,4-dioxane, 160 °C (microwave), 20 min, 5–24%.

The R¹ position

The initial rounds of medicinal chemistry demonstrated that changes to the R¹ group were tolerated and that the cyclohexyl ring of 12 was slightly more active than the initial α -methylbenzyl group of 1. To complete the exploration of the R¹ group, an optimisation array was conducted, maintaining a phenyl ring at the R² position for reference. 3-Bromo-5-phenylpyrazine-2-amine 35 was prepared from 3-amino-6-bromopyrazine-2-carboxylic acid 34 in two steps (Scheme 3). Displacement of the 3-bromo group followed by cyclisation with CDI gave compounds 36–42. Truncation of 1 to an isopropyl group (in 36) resulted in a 10-fold drop in activity while rigidification by replacement of cyclohexyl with an aromatic ring (in 37) resulted in a complete loss of activity (Table 7). The majority of changes were designed to introduce polar solubilising groups. Alkyl ethers 38 and 39 showed only two- and fivefold losses of activity, respectively. Alkoxy compound 40 was ~10-fold less active than the cyclohexyl, whereas the basic compounds 41 and 42 showed poor anti-trypanosomal activity.

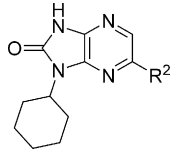
Both 28 and 38 showed decreased protein binding relative to 1 (7.2 and 15% unbound, respectively, versus 0.3% unbound) and improved solubility (> 250 and 55 μ M, respectively, compared with

Table 5. Variation of the R³, R⁴, and R⁵ groups of compound 19.

ID	R ³	R ⁴	R ⁵	PPB [% free]	clog <i>P</i>	EC ₅₀ [μ M] ^[a]		Aq. Sol. [μ M] ^[b]
						<i>T. b. brucei</i>	MRC5	
19	H	H	H	0.8	3.9	0.04	> 50	110
20	OMe	H	H	0.7	3.8	0.33	24	ND
21	CH ₂ OH	H	H	4.7	2.9	0.4	> 50	ND
22	C(O)NHMe	H	H	ND	2.9	1.7	> 50	ND
23	CH ₂ NMe ₂	H	H	ND	3.8	5	> 50	ND
24	H	CH ₂ OH	H	ND	2.9	0.03	> 50	> 250
25	H	NHCOMe	H	ND	3.2	0.9	> 50	ND
26	H	H	F	0.7	3.9	0.06	> 50	20
27	H	H	OMe	ND	3.9	0.9	> 50	ND
28	H	H	CH ₂ OH	7.2	2.9	0.05	> 50	> 250

[a] Values are the geometric mean of two or more determinations; standard deviation is typically within 2-fold of the EC₅₀ value. [b] Aqueous kinetic solubility. ND: not determined.

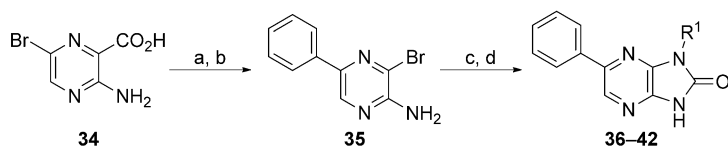
Table 6. Variation of the R² group of compound 19.



ID	R ²	clogP	EC ₅₀ [μM] ^[a] <i>T. b. brucei</i>	MRC5	Aq. Sol. [μM] ^[b]
19		3.9	0.04	> 50	110
29		3.0	0.07	> 50	ND
30		3.0	0.1	> 50	ND
31		3.5	0.08	> 50	ND
32		2.3	0.05	> 50	220
33		2.3	2	> 50	ND

[a] Values are the geometric mean of two or more determinations; standard deviation is typically within 2-fold of the EC₅₀ value. [b] Aqueous kinetic solubility. ND: not determined.

< 12 μM). However, both compounds were less metabolically stable when incubated with mouse hepatic microsomes ($CL_{int} = 2.4$ and $1.6 \text{ mL min}^{-1} \text{ g}^{-1}$, respectively, versus $< 0.5 \text{ mL min}^{-1} \text{ g}^{-1}$) but still progressable. Given these results, both **28** and **38** were progressed into in vivo PK studies. Compound **28** showed significantly higher levels of exposure relative to **38**. Compound **28** also exhibited an improvement in the time to reach C_{max} compared to **1** (15 min versus 2 h) when dosed orally (Table 8), presumably a result of its improved solubility. However, **28** was cleared quite rapidly after both oral and i.p. administration, likely due to the higher metabolic instability of the compound; it would be unlikely to deliver sufficient duration of efficacious free drug concentration at a tolerated dose. We decided to investigate alternative scaffolds with the aim of improving metabolic stability and solubility.

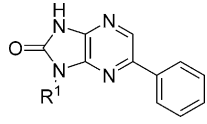


Scheme 3. Reagents and conditions: a) phenylboronic acid, Pd(PPh₃)₄, K₂CO₃ (2 M aqueous), DMF, 140 °C (microwave), 10 min, 100%; b) NaOAc, AcOH, Br₂, RT, 16 h, 63%; c) amine, DIPEA, *n*BuOH, 220 °C (microwave), 1 h; d) CDI, dioxane, 130 °C (microwave), 10 min, 2–71% over two steps.

Scaffold hopping: the core group

Initial work was conducted to investigate the importance of the pyrazine nitrogen atoms (by removal of both of them,

Table 7. Variation of the R¹ group of compound 19.



ID	R ¹	clogP	EC ₅₀ [μM] ^[a] <i>T. b. brucei</i>	MRC5	Aq. Sol. [μM] ^[b]
19		3.9	0.04	> 50	110
36		2.5	0.3	> 50	ND
37		2.9	> 50	> 50	ND
38		2.3	0.1	> 50	55
39		2.0	0.2	> 50	ND
40		1.7	0.5	> 50	ND
41		1.7	13	> 50	ND
42		2.4	2	> 50	ND

[a] Values are the geometric mean of two or more determinations; standard deviation is typically within 2-fold of the EC₅₀ value. [b] Aqueous kinetic solubility. ND: not determined.

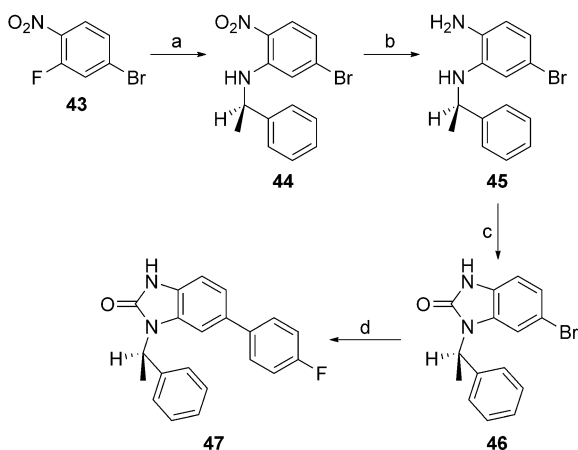
Table 8. PK data for compounds 1, 28, and 38.

ID	Route	Dose [mg kg ⁻¹]	C _{max} [ng mL ⁻¹] ^[a]	t _{max} [h] ^[b]	AUC ₍₀₋₈₎ [ng min mL ⁻¹] ^[c]	t _{1/2} [h] ^[d]
1	p.o.	5	110	4	36 000	3
28	i.p.	20	5200	0.083	230 000	1.2
28	p.o.	20	910	0.25	69 000	1.7
38	i.p.	20	83	2	22 000	2.2

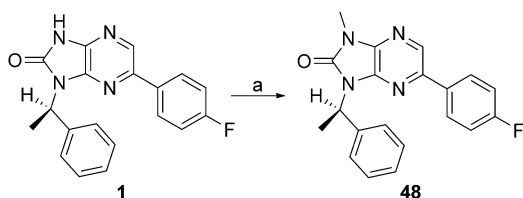
[a] Maximum concentration reached. [b] Time after initial dose at which C_{max} was reached. [c] Area under the curve. [d] Half-life of compound in the blood.

Scheme 4). Thus, 1-bromo-3-fluoro-4-nitrophenyl **43** was reacted with α-methylbenzyl amine to give intermediate **44** (Scheme 4). The nitro group was reduced, then **45** was cyclised with CDI to give (*R*)-6-bromo-1-(1-phenylethyl)-1*H*-benzo[*d*]imidazol-2(3*H*)-one (**46**). Finally a cross-coupling reaction gave the desired compound **47**. Removal of both ring nitrogen atoms of **1** (EC₅₀: 0.08 μM) to give **47** (EC₅₀: 10 μM) resulted in a 100-fold loss of activity, indicating that one or both of the pyrazine nitrogen atoms are important.

Capping the imidazo NH group of **1** with a methyl group gave **48**, leading to a 100-fold loss of activity (EC₅₀: 8 μM versus 0.08 μM for **48** and **1**, respectively), suggesting the importance of the imidazole NH (Scheme 5). To probe the



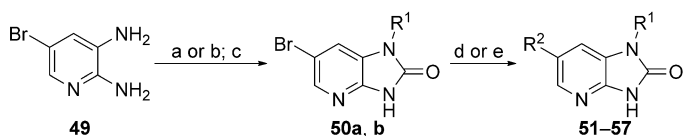
Scheme 4. Reagents and conditions: a) (*R*)-methylbenzylamine, Cs₂CO₃, DMF, 120 °C; b) charcoal (200% w/w), NaBH₄, THF, H₂O, RT, 16 h, 34% over two steps; c) CDI, 1,4-dioxane, 140 °C, 20 min, 61%; d) Pd(PPh₃)₄ (5 mol%), K₂CO₃ (1.5 M aqueous), boronic acid, DMF, 140 °C, 5 min, 44%.



Scheme 5. Reagents and conditions: a) NaH, MeI, DMF, RT, 3 h, 38%.

effect of the N7 nitrogen, a series of compounds were made in which the N7 nitrogen atom was replaced with CH, along with a variety of substituents at the N1- and 6-positions. 2,3-Diamino-5-bromopyridine **49** was subjected to either reductive amination or alkylation conditions to introduce the N3 substituent, followed by cyclisation with CDI to afford the key 6-bromo-1-(*R*)-1*H*-imidazo[4,5-*b*]pyrazin-2(3*H*)-one scaffold **50a–b** (Scheme 6). Treatment of this under either Suzuki or Buchwald conditions afforded desired 6-substituted analogues (**51–57**).

Removal of N7 was tolerated if R¹ was retained as cyclohexyl (**51**) and R² was retained as a phenyl ring (Table 9). Replacement of the phenyl group at R² with a piperidine (**56**) was also tolerated. However, introduction of either 3-pyridyl- (**55**), morpholino- (**57**), or (2-hydroxymethyl)phenyl groups (**53**) gave rise to compounds that were approximately 2-, 7- and 13-fold less active than their N7 homologues (**30**, **32**, and **28**, respec-



Scheme 6. Reagents and conditions: a) 1) cyclohexanone, AcOH, CH₂Cl₂; 2) Na(OAc)₃BH, 63%; b) PhC(CH₃)₂Cl, Et₃N, THF, 9%; c) CDI, MeCN, 69–90%; d) ArB(OR)₂, K₃PO₄, Pd(PPh₃)₄, DMF/H₂O (3:1), 130 °C (microwave), 3–69% (compounds **51–55**); e) (*S*)-PHOS, tBuONa, (R²)₂NH, Pd₂dba₃, toluene, 120 °C (microwave), 32–47% (compounds **56–57**).

Table 9. Replacement of N7 nitrogen.

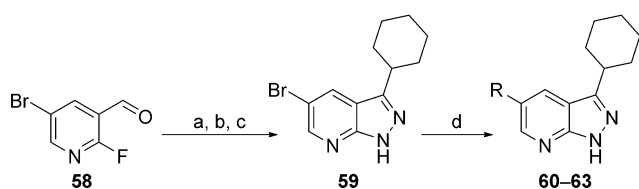
ID	R ¹	R ²	clogP	EC ₅₀ [μM] ^[a]		Aq. Sol. [μM] ^[b]
				<i>T. b. brucei</i>	MRC5	
51			3.9	0.054	> 50	36
52			3.1	0.79	23	ND
53			2.8	0.67	> 50	ND
54			3.2	15	> 50	ND
55			2.8	0.23	> 50	180
56			3.3	0.093	> 50	> 250
57			2.2	0.33	> 50	ND

[a] Values are the geometric mean of two or more determinations; standard deviation is typically within 2-fold of the EC₅₀ value. [b] Aqueous kinetic solubility. ND: not determined.

tively). At the R¹ position, replacement with 2-phenylpropan-2-yl groups (**52**, **54**) was less favourable.

It was hypothesised that the “urea” moiety may be a cause of the poor solubility, possibly through its ability to cause anti-parallel hydrogen bonded dimers. However, if this was to be replaced, certain features would need to be retained: the carbonyl group could act as a hydrogen bond acceptor, and the NH group as a hydrogen bond donor. As N1 was a tertiary nitrogen it was hypothesised that does not make any important interactions and could be replaced by a carbon atom. This would then allow the carbonyl to be replaced by a nitrogen, which could also act as a hydrogen bond acceptor, giving an aza-indazole scaffold: a known kinase scaffold.

The key intermediate 5-bromo-3-cyclohexyl-1*H*-pyrazolo[3,4-*b*]pyridine **59** was synthesised in three steps from commercially available 5-bromo-2-fluoronicotinaldehyde **58** and was subsequently reacted under Suzuki conditions to give the corresponding 5-aryl-/heteroaryl-substituted compounds **60–63** (Scheme 7). Both phenyl (**60**) and 3-pyridyl (**63**) were tolerated, with the former showing similar levels of potency and selectivity to the other core scaffolds bearing an unsubstituted phenyl group (**51** EC₅₀ = 0.054 μM and **19** EC₅₀ = 0.04 μM; Table 10). Phenyl groups (**61** and **62**) bearing a substituent at the 2-position were less favourable.



Scheme 7. Reagents and conditions: a) cyclohexylmagnesium bromide, THF, $-78\text{ }^{\circ}\text{C} \rightarrow \text{RT}$, 55%; b) PDC, CH_2Cl_2 , $0\text{ }^{\circ}\text{C} \rightarrow \text{RT}$, 91%; c) $\text{NH}_2\text{NH}_2 \cdot \text{H}_2\text{O}$, EtOH, reflux, 95%; d) RB(OH)_2 , 2 M Na_2CO_3 , $\text{Pd(PPh}_3)_4$, DME/ H_2O /EtOH (7:3:2), $140\text{ }^{\circ}\text{C}$, microwave, 16–69%.

Table 10. SAR for aza-indazoles.

ID	R	clogP	EC_{50} [μM] ^[a] <i>T. b. brucei</i>	MRC5	Aq. Sol. [μM] ^[b]
60		4.7	0.059	> 50	20
61		3.6	1.3	> 50	ND
62		4.7	2.6	> 50	ND
63		3.5	0.26	> 50	250

[a] Values are the geometric mean of two or more determinations; standard deviation is typically within 2-fold of the EC_{50} value. [b] Aqueous kinetic solubility. ND: not determined.

Table 11. In vitro ADMET data.

ID	R ¹	X	EC_{50} [μM] ^[a] <i>T. b. brucei</i>	MRC5	CL_{int} [$\text{mL min}^{-1} \text{g}^{-1}$]	PPB [% free]	Aq. Sol. [μM] ^[b]	tPSA [\AA^2]
28	(2- CH_2OH)Ph	N	0.046	> 50	2.4	7.2	> 250	83
19	Ph	N	0.044	> 50	3.6	0.8	ND	64
51	Ph	CH	0.054	> 50	5.8	2.9	36	51
30	3-pyridyl	N	0.12	> 50	2.8	2.3	ND	76
55	3-pyridyl	CH	0.23	> 50	2.7	11	180	64
31	piperidine	N	0.077	> 50	15	0	ND	67
56	piperidine	CH	0.093	> 50	3.6	11	> 250	54
60	–	CH	0.059	> 50	15	1.4	20	42
63	–	N	0.26	> 50	6.6	5.2	250	54

[a] Values are the geometric mean of two or more determinations; standard deviation is typically within 2-fold of the EC_{50} value. [b] Aqueous kinetic solubility. ND: not determined.

Removal of one the nitrogen atoms from the pyrazine ring was predicted to lead to improvements in metabolic stability, protein binding, and solubility (Table 11). However, replacement of the core scaffold with the aza-indazole had a negative effect on the in vitro DMPK properties of the compounds (compare **51** and **60**; **55** and **63**).

Compound **56** was selected for in vivo PK studies, as it had the most favourable in vitro profile (potency, metabolic stability, protein binding, and solubility). However, **56** had lower exposure levels than **28** and was also cleared rapidly, in line with its higher CL_{int} value (Table 12).

Table 12. PK data for compounds **28** and **56**.

ID	Route	Dose [mg kg^{-1}]	C_{max} [ng mL^{-1}] ^[a]	t_{max} [h] ^[b]	$\text{AUC}_{(0-8)}$ [ng min mL^{-1}] ^[c]	$t_{1/2}$ [h] ^[d]
28	i.p.	20	5200	0.083	230 000	1.2
56	i.p.	10	580	0.25	53 000	0.7

[a] Maximum concentration reached. [b] Time after initial dose at which C_{max} was reached. [c] Area under the curve. [d] Half-life of compound in the blood.

Determination of the mode of the antiparasitic effect: static or cidal action

During the course of these studies, work from parallel series indicated that compounds that are cytostatic against *T. brucei* are not effective in animal models of infection. Therefore compounds that only exert a static effect (i.e., stopping the growth of cells, whilst not killing them) or a decrease in growth rate are unlikely to clear the parasites completely and should be removed from drug discovery pipelines as early as possible. To provide information regarding the mode of action of the compounds discussed, we selected a number of examples to run in a static–cidal assay.^[22,26] Compounds with either an imidazo[4,5-*b*]pyrazin-2(3*H*)-one (**24**, **26**, **28**, **30**, and **39**) or imidazo[4,5-*b*]pyridin-2(3*H*)-one (**51**, **55**, and **56**) core showed growth-slowing or static behaviour at all concentrations tested, whereas compounds containing a 1*H*-pyrazolo[3,4-*b*]pyridine core (**60** and **63**) showed cidal behaviour at a minimum cidal concentration of $17\text{ }\mu\text{M}$ (Table 13). With the exception of pentamidine and melarsoprol, all compounds showed either biphasic dose–response curves or partial curves. This suggested these compounds may act on at least two targets, the first of which caused a growth-slowing or static mode of action, whilst inhibition of the subsequent target(s) had a cytotoxic effect (Figure 1). Only pentamidine, melarsoprol, **60**, and **63** reached a well-defined plateau at 100% inhibition, which explains why only these compounds showed clear cidal activity.

The mode(s) of action of these compounds are not known. Analysis of the literature suggests that these chemotypes have been investigated against many families of enzyme in humans, including protein kin-

ID	<i>T. b. brucei</i> EC ₅₀ [μM] ^[a]	MCC [μM] ^[b]	SCEC ₅₀ (1) [μM] ^[b]	SCEC ₅₀ (2) [μM] ^[b]	Mode ^[c]
24	0.03	> 50	0.07	30	S
26	0.06	> 50	0.09	–	GS
28	0.05	> 50	0.10	> 50	GS
30	0.12	> 50	0.23	–	GS
39	0.20	> 50	0.41	32	S
51	0.05	> 50	0.02	41	S ^[d]
55	0.23	> 50	0.33	–	GS
56	0.09	> 50	0.07	> 50	GS
60	0.06	17	0.08	7.9	C
63	0.26	17	0.28	6.1	C
pentamidine	0.004	0.1	0.019	–	C
melaersoprol	0.009	0.1	0.031	–	C

[a] Values determined by the standard *T. brucei* cell viability assay and are the geometric mean of two or more determinations; standard deviation is typically within 2-fold of the EC₅₀ value. [b] Compounds were also tested in the static–cidal assay carried out in triplicate to determine minimal cidal concentration (MCC) and static cidal EC₅₀ values for the first [SCEC₅₀(1)] and second [SCEC₅₀(2)] sites. EC₅₀ and SCEC₅₀(1) are expected to represent the same mode of action of the compounds and are therefore very similar.^[26] [c] GS: growth-slowing, S: static, C: cidal. [d] Indication of cidality at 50 μM.

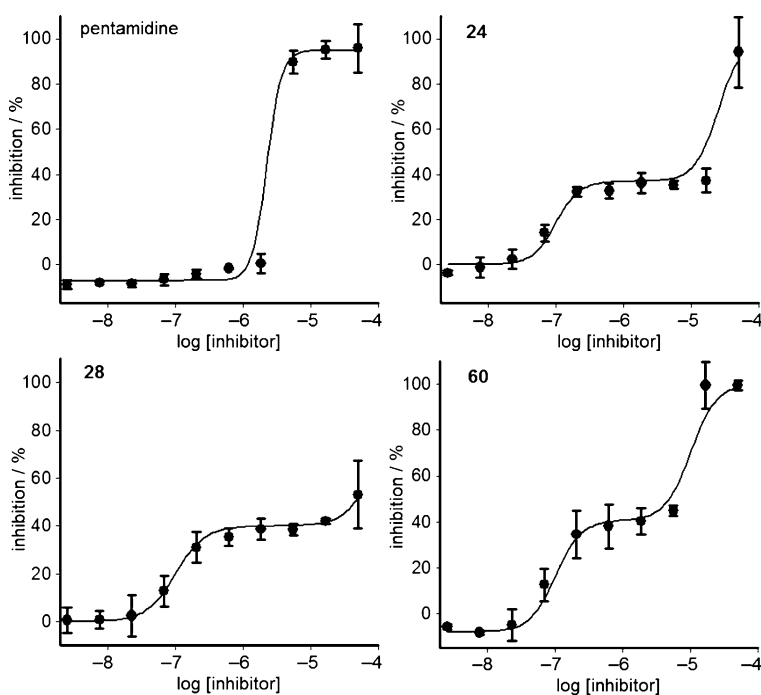


Figure 1. Static/cidal dose–response curves for pentamidine, **24**, **28**, and **60**. Data are the average of triplicate measurements after 48 h incubation of *T. b. brucei* cells with a) pentamidine (cidal), b) compound **24** (static at concentration tested), c) compound **28** (growth-slowing), and d) compound **60** (cidal). Inhibitors were tested in a 10-point dose–response curve at a 1:3 dilution factor; data were analysed with either a monophasic or a biphasic fit. Static and cidal are defined by analysis of the growth curves as shown in the Supporting Information (Figure S4), where cidal compounds show a decrease in the numbers of parasites.

ases,^[27–32] hydrolases,^[33] and transferases.^[34] Our work described in Figure 1 suggests that there are likely to be several modes of action in trypanosomes.

Given our experience from other programmes, in order for a compound to show efficacy in a mouse model of HAT, it is important that the compound is cidal, rather than static, in its activity against *T. brucei*. Compounds that are consistent with this are **60** and **63**. However, given their metabolic instability and poor potency (minimum cidal concentrations of 17 μM), it is highly unlikely that either would deliver efficacy in a mouse model of HAT. Further work is needed to improve the potency and pharmacokinetic properties of the molecules.

Conclusions

Through our phenotypic screening approach with a relatively small library, we have developed a series of compounds that exhibit good levels of potency in the *T. b. brucei* growth inhibition assay, and that are nontoxic to MRC5 mammalian cells. Despite the fact that the screening library was a focused protein kinase library, it was possible to obtain compounds with selectivity over the mammalian protein kinases assayed. These compounds possess reasonable physicochemical properties and show oral exposure, but have modest half-lives. By changing the substituents R¹ and R² it was possible to optimise the compounds for potency and to alter key physicochemical and DMPK properties, in the absence of knowledge of the molecular target. It was also possible to scaffold-hop, although it is possible that the new scaffold works on a different molecular target.

The ultimate aim would be to devise a compound that has oral bioavailability and the capacity to penetrate the BBB. The compounds prepared in this study generally have physicochemical properties consistent with BBB penetration as reported by Wager,^[19] in terms of *M_r*, tPSA, clog*P*, and number of hydrogen bond donors. Although of course for compounds taken forward, BBB permeability would have to be determined experimentally.

Key compounds in a static–cidal assay showed an unusual biphasic nature, giving two points of inflection on the dose–response curve. This suggests at least two modes of action (or, less likely due to the use of a clonal line, differential susceptibility of cell sub-populations). Compounds from the 1*H*-imidazo[4,5-*b*]pyrazin-2(3*H*)-one scaffold appeared to be either static or growth-slowing, whilst compounds from the 1*H*-pyrazolo[3,4-*b*]pyridine series were cidal. It is possible that compounds from the 1*H*-imidazo[4,5-*b*]pyrazin-2(3*H*)-one scaffold will be cidal at higher concentrations, and that the key difference between the two scaffolds is not a difference in mode-of-action but a difference in potency against the target(s) represented by the second phase of the biphasic curves.

A way forward would be to identify the molecular target(s) of the compounds, specifically which target(s) causes the cytotoxic activity, and to focus efforts on potent inhibition of this target. Subsequent progression of the series will require identification of compounds that are cytotoxic.

dal. It will also be necessary to optimise the key properties of the molecule (microsomal stability, solubility, and protein binding). Although it has proved possible to optimise the compound in terms of potency and to some extent at least the pharmacokinetic parameters, we have reached a biological issue which has proved difficult to resolve in the absence of knowledge of the target. In this case, a combination of phenotypic and target-based approaches would probably be optimal.

Experimental Section

Chemistry

Compounds **1**, **2**, **3** and **13** were purchased from BioFocus. Chemicals and solvents were purchased from Aldrich Chemical Co., Fluka, ABCR, VWR, Acros, Fisher Chemicals, and Alfa Aesar and were used as received unless otherwise stated. Air- and moisture-sensitive reactions were carried out under an inert atmosphere of argon in oven-dried glassware. Analytical thin-layer chromatography (TLC) was performed on pre-coated TLC plates (layer 0.20 mm silica gel 60 with fluorescent indicator UV254, Merck). Developed plates were air dried and analyzed under a UV lamp (λ 254/365 nm). Flash column chromatography was performed using pre-packed silica gel cartridges (230–400 mesh, 40–63 μ m, SiliCycle) (unless otherwise stated) using a Teledyne ISCO Combiflash Companion or Combiflash Retrieve. ^1H and ^{13}C NMR spectra were recorded on a Bruker Avance II 500 spectrometer (^1H at 500.1 MHz, ^{13}C at 125.8 MHz), or a Bruker DPX300 spectrometer (^1H at 300.1 MHz). Chemical shifts (δ) are expressed in ppm recorded using the residual solvent as internal reference in all cases. Signal splitting patterns are described as singlet (s), doublet (d), triplet (t), quartet (q), pentet (p), multiplet (m), broad (br), or a combination thereof. Coupling constants (J) are quoted to the nearest 0.1 Hz. LC–MS analyses were performed with either an Agilent HPLC 1100 series instrument connected to a Bruker Daltonics MicroTOF or an Agilent Technologies 1200 series HPLC connected to an Agilent Technologies 6130 quadrupole spectrometer, where both instruments were connected to an Agilent diode array detector. LC–MS chromatographic separations were conducted with a Waters Xbridge C_{18} column, 50 mm \times 2.1 mm, 3.5 μ m particle size; mobile phase: $\text{H}_2\text{O}/\text{MeCN} + 0.1\%$ HCOOH, or $\text{H}_2\text{O}/\text{MeCN} + 0.1\%$ NH_3 ; linear gradient from 80:20 to 5:95 over 3.5 min and then held for 1.5 min; flow rate: 0.5 mL min^{-1} . All tested compounds had a measured purity of $\geq 95\%$ (by TIC [total ion current] and UV) as determined by this analytical LC–MS system. High-resolution electrospray MS measurements were performed on a Bruker Daltonics MicroTOF mass spectrometer. Microwave-assisted chemistry was performed using a Biotage initiator microwave synthesiser.

1-Benzyl-6-(4-fluorophenyl)-1H-imidazo[4,5-b]pyrazin-2(3H)-one (9): A mixture of 3,5-dibromopyrazin-2-amine (400 mg, 1.58 mmol), benzylamine (189 μ L, 1.74 mmol) and DIPEA (302 μ L, 1.74 mmol) in EtOH (2 mL) was heated under microwave irradiation at 180 °C for 90 min. The reaction was cooled to room temperature and concentrated in vacuo. The resulting slurry was partitioned between CH_2Cl_2 (20 mL) and H_2O (10 mL), the organic layer was washed with brine (10 mL) and concentrated in vacuo. The resultant crude residue was purified by column chromatography, eluting with 20% EtOAc/hexane to give N2-benzyl-6-bromopyrazine-2,3-diamine (**6c**; 281 mg, 64%) as a brown oil. Compound **6c** (281 mg, 1.10 mmol), 4-fluorophenylboronic acid (154 mg, 1.10 mmol), tetrakis(triphenylphosphine)palladium(0) (58 mg, 0.05 mmol), potassium carbonate

(414 mg, 3.0 mmol) in H_2O (5 mL), and DMF (5 mL) were combined and heated under microwave irradiation at 160 °C for 5 min. The reaction was then cooled to room temperature, and then diluted with a 10:1 mixture of $\text{CH}_2\text{Cl}_2/\text{MeOH}$ (10 mL). The mixture was poured onto an SCX-2 column and allowed to drip through; it was then washed with a 10:1 mixture of $\text{CH}_2\text{Cl}_2/\text{MeOH}$ (10 mL). The SCX-2 column was then eluted with NH_3 in MeOH (7 N, 20 mL) and the eluates were concentrated in vacuo. The resultant brown solid was dissolved in 1,4-dioxane (2 mL), and CDI (140 mg, 0.86 mmol) was added. The mixture was heated under microwave irradiation at 140 °C for 20 min, cooled to room temperature and concentrated in vacuo. The resultant crude residue was purified by column chromatography, eluting with 0–100% EtOAc/petroleum ether (PE) 40–60 °C to give the title compound **9** (47 mg, 15%) as an off-white solid. ^1H NMR (500 MHz, $[\text{D}_6]\text{DMSO}$): δ = 12.19 (s, 1 H), 8.53 (s, 1 H), 8.09–8.06 (brs, 2 H), 7.43–7.27 (m, 7 H), 5.08 ppm (s, 2 H); LRMS (ES+): m/z (%) 321.0 $[\text{M} + \text{H}]^+$ (100); HRMS (m/z): $[\text{M} + \text{H}]^+$ calcd for $\text{C}_{18}\text{H}_{14}\text{FN}_4\text{O}$: 321.1146, found: 321.1131.

(R)-6-Phenyl-1-(1-phenylethyl)-1H-imidazo[4,5-b]pyrazin-2(3H)-one (14): (R)-6-bromo-N²-(1-phenylethyl)pyrazine-2,3-diamine (**6a**; 100 mg, 0.35 mmol), phenyl boronic acid (44 mg, 0.35 mmol), tetrakis(triphenylphosphine)palladium(0) (20 mg, 0.018 mmol), potassium carbonate (700 μ L of a 1.5 M solution in H_2O , 1.05 mmol), and DMF (2 mL) were combined and heated under microwave irradiation at 160 °C for 5 min. The reaction was then cooled to room temperature, and then diluted with a 10:1 mixture of $\text{CH}_2\text{Cl}_2/\text{MeOH}$ (10 mL). The mixture was poured onto an SCX-2 column and allowed to drip through, then washed with a 10:1 mixture of $\text{CH}_2\text{Cl}_2/\text{MeOH}$ (10 mL). The SCX-2 column was then eluted with NH_3 in MeOH (7 N, 20 mL), and the eluates were concentrated in vacuo. The resultant brown solid was dissolved in 1,4-dioxane (2 mL), and CDI (140 mg, 0.86 mmol) was added. The mixture was heated under microwave irradiation at 140 °C for 20 min, cooled to room temperature and concentrated in vacuo. The resultant crude residue was purified by column chromatography, eluting with 0–100% EtOAc/PE 40–60 °C to give the title compound **14** (21 mg, 18%) as a pale-yellow solid. ^1H NMR (500 MHz, $[\text{D}_6]\text{DMSO}$): δ = 12.12 (s, 1 H), 8.51 (s, 1 H), 8.00 (d, J = 7.3 Hz, 2 H), 7.55–7.47 (m, 4 H), 7.42–7.34 (m, 3 H), 7.27 (t, J = 7.3 Hz, 1 H), 5.74 (q, J = 7.2 Hz, 1 H), 2.03 ppm (d, J = 7.3 Hz, 3 H); LRMS (ES+): m/z (%) 317.1 $[\text{M} + \text{H}]^+$ (97); HRMS (m/z): $[\text{M} + \text{H}]^+$ calcd for $\text{C}_{19}\text{H}_{17}\text{N}_4\text{O}$: 317.1397, found: 317.1394.

1-Cyclohexyl-6-(4-fluorophenyl)-1H-imidazo[4,5-b]pyrazin-2(3H)-one (12): 6-Bromo-1-cyclohexyl-1H-imidazo[4,5-b]pyrazin-2(3H)-one (**7b**) (100 mg, 0.33 mmol), tetrakis(triphenylphosphine)palladium(0) (12 mg, 0.01 mmol), potassium carbonate (0.65 mL of a 1.5 M solution in H_2O , 1.0 mmol), 4-fluorophenyl boronic acid (46 mg, 0.33 mmol), in DMF (2.0 mL) were combined and the mixture was heated under microwave irradiation at 180 °C for 5 min. The reaction mixture was absorbed onto silica and purified by chromatography eluting with 50% EtOAc/PE 40–60 °C to give the title compound **12** (17 mg, 16%) as a yellow solid. ^1H NMR (500 MHz, $[\text{D}_6]\text{DMSO}$): δ = 12.04 (s, 1 H), 8.49 (s, 1 H), 8.10–8.07 (m, 2 H), 7.34 (t, J = 8.8 Hz, 2 H), 4.28–4.22 (m, 1 H), 2.37–2.29 (m, 2 H), 1.88–1.80 (m, 4 H), 1.71 (d, J = 12.8 Hz, 1 H), 1.44–1.36 (m, 2 H), 1.29–1.22 ppm (m, 1 H); LRMS (ES+): m/z (%) 313.2 $[\text{M} + \text{H}]^+$ (100); HRMS (m/z): $[\text{M} + \text{H}]^+$ calcd for $\text{C}_{17}\text{H}_{18}\text{FN}_4\text{O}$: 313.1459, found: 313.1458.

1-Cyclohexyl-6-(piperidin-1-yl)-1H-imidazo[4,5-b]pyrazin-2(3H)-one (31): 6-Bromo-1-cyclohexyl-1H-imidazo[4,5-b]pyrazin-2(3H)-one (100 mg, 0.33 mmol), tris(dibenzylideneacetone)dipalladium (16 mg, 0.017 mmol), potassium *tert*-butoxide (114 mg, 1.0 mmol), (\pm)-2,2'-bis(diphenylphosphino)-1,1'-binaphthyl (22 mg, 0.034 mmol), piperidine (67 μ L, 0.68 mmol) and 1,4-dioxane

(2.0 mL) were combined and heated under microwave irradiation at 180 °C for 5 min. The reaction was cooled to room temperature, absorbed onto silica and purified by column chromatography, eluting with 50% EtOAc/hexane to give the title compound **31** (25 mg, 24%) as a yellow solid. ¹H NMR (500 MHz, [D₆]DMSO): δ = 11.36 (s, 1H), 7.45 (s, 1H), 4.16–4.09 (m, 1H), 3.38–3.32 (m, 2H), 2.52–2.50 (m, 2H), 2.27–2.19 (m, 2H), 1.83 (d, *J* = 13.0 Hz, 2H), 1.73–1.67 (m, 3H), 1.59 (brs, 6H), 1.39–1.31 (m, 2H), 1.21–1.13 ppm (m, 1H); LRMS (ES+): *m/z* (%) 302.2 [M+H]⁺ (100); HRMS (*m/z*): [M+H]⁺ calcd for C₁₆H₂₄N₅O: 302.1975, found: 302.1973.

1-(1-Methoxypropan-2-yl)-6-phenyl-1H-imidazo[4,5-b]pyrazin-2(3H)-one (39): 3-Bromo-5-phenylpyrazine-2-amine (125 mg, 0.5 mmol), 1-methoxybutan-2-amine (77 mg, 0.75 mmol), DIPEA (0.1 mL), and *n*BuOH (0.5 mL) were heated under microwave irradiation at 220 °C for 1 h. The reaction was diluted with EtOAc (10 mL), washed with H₂O (3 × 10 mL), the organic layer dried over MgSO₄, filtered, and the solvent was removed in vacuo. Column chromatography eluting with CH₂Cl₂ to CH₂Cl₂/MeOH (95:5) afforded the desired substituted 6-phenylpyrazine-2,3-diamine, which was used for subsequent reaction without further purification. Substituted 6-phenylpyrazine-2,3-diamine (0.5 mmol), CDI (97 mg, 0.6 mmol), and 1,4-dioxane (1 mL) were heated under microwave irradiation at 130 °C for 10 min. The crude reaction mixture was partitioned between EtOAc and H₂O, the organic layer was dried over MgSO₄, filtered, and the solvent removed in vacuo. The resultant crude residue was purified by column chromatography, eluting with EtOAc to give the title compound **39** (13 mg, 10%) as a colourless solid. ¹H NMR (500 MHz, CDCl₃): δ = 8.90 (brs, 1H), 8.41 (s, 1H), 7.99–7.97 (m, 2H), 7.51 (t, *J* = 7.3 Hz, 2H), 7.44 (t, *J* = 7.3 Hz, 1H), 4.98–4.94 (m, 1H), 4.27 (t, *J* = 10.1 Hz, 1H), 3.68 (dd, *J* = 10.1, 5.2 Hz, 1H), 3.37 (s, 3H), 1.65 ppm (d, *J* = 7.1 Hz, 3H); LRMS (ES+): *m/z* (%) 285.1 [M+H]⁺ (100); HRMS (*m/z*): [M+H]⁺ calcd for C₁₅H₁₆N₄O₂: 285.1346; found, 285.1336.

Biological assays

Medium-throughput screen for African trypanosomes and cytotoxicity: Measurement of inhibition of the proliferation of L-6 cells (mouse muscle fibroblasts) and *T. brucei* bloodstream-stage cells was performed as previously described.^[35,36]

Trypanosome and MRC5 proliferation assay: Measurement of inhibition of the proliferation of MRC5 cells (human lung fibroblasts) and *T. brucei* bloodstream-stage cells was performed using a modification of a cell viability assay previously described.^[35,36] Compounds (50 mM to 0.5 nM) were incubated with 2 × 10³ cells per well in 0.2 mL of the appropriate culture medium (MEM with 10% foetal bovine serum for MRC5 cells) in clear 96-well plates. Plates were incubated at 37 °C in the presence of 5% CO₂ for 69 h. Resazurin was then added to a final concentration of 50 μM, and plates were incubated as above for a further 4 h before being read on a BioTek Flx800 fluorescence plate reader.

Determination of cidal activity against *T. brucei* bloodstream-stage cells was performed using a static-cidal (SC) assay as previously reported.^[26] Briefly, bloodstream-form trypanosomes were seeded into 384-well plates at 4 × 10⁵ mL⁻¹ (50 μL per well), followed by immediate addition of resazurin (50 μM final) to one of the plates, and all plates were incubated at 37 °C, 5% CO₂. After 4 h the *t*₀ plate was read using a PerkinElmer Victor 3 plate reader (λ_{ex} = 528 nm, λ_{em} = 590 nm). The second plate was processed in the same manner 20 h later, and at 44 h the last plate was processed. The minimum cidal concentration (MCC) is defined as the lowest concentration of drug that results in a decrease of resorufin signal

over time. For dose–response curves from this assay either a monophasic or a biphasic equation was used, depending on which one provided the best fit. For monophasic fits, the following four-parametric equation [Eq. (1)] was used:

$$y = A + \frac{B-A}{1 + (C/x)^D} \quad (1)$$

in which *A* = percent inhibition at bottom, *B* = percent inhibition at top, *C* = EC₅₀, *D* = slope, *x* = inhibitor concentration, and *y* = percent inhibition. Equation (2) was used for biphasic fits:

$$\frac{A}{1 + 10^{[C-\log(x)] \times B}} + \frac{100-A}{1 + 10^{[D-\log(x)] \times B}} \quad (2)$$

for which *A* = percent inhibition at mid-plateau, *B* = slope, *C* = log[SCEC₅₀(1)], *D* = log[SCEC₅₀(2)]. Thus SCEC₅₀(1) is the EC₅₀ for the first phase of the curve, and SCEC₅₀(2) is that for the second phase. Inhibition at the bottom of the curve is fixed at 0% and at the top, 100%.

Intrinsic clearance experiments: Test compound (0.5 μM) was incubated with female CD1 mouse liver microsomes (Xenotech LLC; 0.5 mg mL⁻¹ 50 mM potassium phosphate buffer, pH 7.4), and the reaction started with the addition of excess NADPH (8 mg mL⁻¹ 50 mM potassium phosphate buffer, pH 7.4). Immediately, at *t*₀, then at 3, 6, 9, 15, and 30 min an aliquot (50 μL) of the incubation mixture was removed and mixed with MeCN (100 μL) to stop the reaction. Internal standard was added to all samples, the samples were centrifuged to sediment precipitated protein, and the plates were then sealed prior to UPLC–MS/MS analysis using a Quattro Premier XE instrument (Waters Corp., USA). Xlfit (IDBS, UK) was used to calculate the exponential decay and consequently the rate constant (*k*) from the ratio of peak area of test compound to internal standard at each time point. The rate of intrinsic clearance [*CL*_{int}, mL min⁻¹ (g liver)⁻¹] of each test compound was then calculated with Equation (3):

$$CL_{int} = k \times V \times (\text{microsomal protein yield}) \quad (3)$$

in which *V* [mL (mg protein)⁻¹] is the incubation volume per mg protein added, and microsomal protein yield is taken as 52.5 mg protein per gram of liver. Verapamil (0.5 μM) was used as a positive control to confirm acceptable assay performance.

Plasma protein binding experiments: In brief, a 96-well equilibrium dialysis apparatus was used to determine the free fraction in plasma for each compound (HT Dialysis LLC, Gales Ferry, CT, USA). Membranes (12–14 kDa cutoff) were conditioned in deionised H₂O for 60 min, followed by conditioning in 80:20 deionised H₂O/EtOH for 20 min, and then rinsed in isotonic buffer before use. Female CD1 mouse plasma was removed from the freezer and allowed to thaw on the day of experiment. Thawed plasma was then centrifuged (Allegra X12-R, Beckman Coulter, USA), spiked with test compound (10 μg g⁻¹), and 150 μL aliquots (*n* = 6 replicate determinations) loaded into the 96-well equilibrium dialysis plate. Dialysis against isotonic buffer (150 μL) was carried out for 5 h in a temperature-controlled incubator at ~37 °C (Barworld Scientific Ltd., UK) using an orbital microplate shaker at 125 rpm (Barworld Scientific). At the end of the incubation period, aliquots of plasma or buffer were transferred to micronic tubes (Micronic B.V., the Netherlands), and the composition in each tube was balanced with control fluid such that the volume of buffer to plasma is the same. Sample extraction was performed by the addition of 400 μL MeCN containing

an appropriate internal standard. Samples were allowed to mix for 1 min and then centrifuged at 3000 rpm in 96-well blocks for 15 min (Allegra X12-R, Beckman Coulter, USA). All samples were analysed by UPLC–MS/MS on a Quattro Premier XE Mass Spectrometer (Waters Corp.). The unbound fraction was determined as the ratio of the peak area in buffer to that in plasma.

Solubility experiments: The kinetic aqueous solubility of the test compounds was measured using laser nephelometry. Compounds were subject to serial dilution from 10 mM to 0.5 mM in DMSO. An aliquot was then mixed with Milli-Q H₂O to obtain an aqueous dilution plate with a final concentration range of 250–12 μM, with a final DMSO concentration of 2.5%. Triplicate aliquots were transferred to a flat-bottomed polystyrene plate which was immediately read on the NEPHELOstar (BMG Lab Technologies). The amount of laser scatter caused by insoluble particulates (relative nephelometry units, RNU) was plotted against compound concentration using a segmental regression fit, with the point of inflection being quoted as the compounds' aqueous solubility (in μM).

In vivo pharmacokinetics in mice: Compounds **1** and **28** were dosed orally by gavage as a solution at 5 mg free base per kg or 20 mg free base per kg, respectively (dose volume: 5 or 10 mL kg⁻¹, dose vehicle: 5% DMSO, 40% PEG400, 55% distilled H₂O) to female NMRI mice (*n* = 3). Compounds **28**, **38**, and **56** were dosed as a bolus solution intraperitoneally at 10 (**56**) or 20 (**28** and **38**) mg free base per kg (dose volume: 10 mL kg⁻¹, dose vehicle: 5% DMSO, 40% PEG400, 55% sterile H₂O) to female NMRI mice (*n* = 3). Female NMRI mice were chosen, as these represent the sex and strain used for the stage-1 and stage-2 HAT efficacy models. Blood samples were taken from each mouse at 5 (i.p. only), 15 and 30 min, 1, 2, 4, 6 and 8 h post-dose and mixed with two volumes of distilled H₂O. After suitable sample preparation, the concentration of each compound in blood was determined by UPLC–MS/MS using a Quattro Premier XE (Waters, USA). Pharmacokinetic parameters were derived from the mean blood concentration time curve using PKsolutions software ver. 2.0 (Summit Research Services, USA).

Ethics: All regulated procedures on living animals were carried out under the authority of a project license issued by the Home Office under the Animals (Scientific Procedures) Act 1986, as amended in 2012 (and in compliance with EU Directive EU/2010/63). License applications will have been approved by the University's Ethical Review Committee (ERC) before submission to the Home Office. The ERC has a general remit to develop and oversee policy on all aspects of the use of animals on University premises and is a sub-committee of the University Court, its highest governing body.

Abbreviations

PPB: plasma protein binding; *CL*_{int}: intrinsic clearance; MCC: minimum cidal concentration; SC: static/cidal; NBS: *N*-bromosuccinimide; DIPEA: *N,N*-diisopropylethylamine; CDI: 1,1'-carbonyldiimidazole; DMF: *N,N*-dimethylformamide; THF: tetrahydrofuran; (S)-PHOS: 2-dicyclohexylphosphino-2',6'-dimethoxybiphenyl; *rac*-binap: (±)-2,2'-bis(diphenylphosphino)-1,1'-binaphthyl.

Acknowledgements

Funding for this work was provided by the Wellcome Trust (Grant Ref. WT077705 and Strategic Awards WT083481 and WT100476). We thank Gina McKay (University of Dundee) for performing

HRMS analyses, Lars Sandberg (University of Dundee) for literature analysis, and Daniel James (University of Dundee) for data management.

Keywords: cidal · kinases · phenotypic · static · *Trypanosoma brucei*

- [1] M. P. Barrett, D. W. Boykin, R. Brun, R. R. Tidwell, *Br. J. Pharmacol.* **2007**, *152*, 1155–1171.
- [2] R. Brun, R. Don, R. T. Jacobs, M. Z. Wang, M. P. Barrett, *Future Microbiol.* **2011**, *6*, 677–691.
- [3] P. Cohen, *Nat. Rev. Drug Discovery* **2002**, *1*, 309–315.
- [4] M. Parsons, E. A. Worthey, P. N. Ward, J. C. Mottram, *BMC Genomics* **2005**, *6*, 127.
- [5] C. Naula, M. Parsons, J. C. Mottram, *Biochim. Biophys. Acta Proteins Proteomics* **2005**, *1754*, 151–159.
- [6] C. Doerig, *Biochim. Biophys. Acta Proteins Proteomics* **2004**, *1697*, 155–168.
- [7] J. A. Frearson, P. G. Wyatt, I. H. Gilbert, A. H. Fairlamb, *Trends Parasitol.* **2007**, *23*, 589–595.
- [8] P. G. Wyatt, I. H. Gilbert, K. D. Read, A. H. Fairlamb, *Curr. Top. Med. Chem.* **2011**, *11*, 1275–1283.
- [9] T. C. Hammarton, S. Kramer, L. Tetley, M. Boshart, J. C. Mottram, *Mol. Microbiol.* **2007**, *65*, 1229–1248.
- [10] L. A. T. Cleghorn, A. Woodland, I. Collie, L. Torrie, N. Norcross, T. Luksch, C. Mpamhanga, R. G. Walker, J. C. Mottram, R. Brenk, J. A. Frearson, I. H. Gilbert, P. G. Wyatt, *ChemMedChem* **2011**, *6*, 2214–2224.
- [11] I. H. Gilbert, *J. Med. Chem.* **2013**, *56*, 7719–7726.
- [12] I. H. Gilbert, D. Leroy, J. A. Frearson, *Curr. Top. Med. Chem.* **2011**, *11*, 1284–1291.
- [13] D. C. Swinney, J. Anthony, *Nat. Rev. Drug Discovery* **2011**, *10*, 507–519.
- [14] D. C. Swinney, *Clin. Pharmacol. Ther.* **2013**, *93*, 299–301.
- [15] R. Diaz, S. A. Luengo-Arratta, J. D. Seixas, E. Amata, W. Devine, C. Cordon-Obras, D. I. Rojas-Barros, E. Jimenez, F. Ortega, S. Crouch, G. Colmenarejo, J. M. Fiandor, J. J. Martin, M. Berlanga, S. Gonzalez, P. Manzano, M. Navarro, M. P. Pollastri, *PLoS Neglected Trop. Dis.* **2014**, *8*, e3253.
- [16] I. Peña, M. Pilar Manzano, J. Cantizani, A. Kessler, J. Alonso-Padilla, A. I. Bardera, E. Alvarez, G. Colmenarejo, I. Cotillo, I. Roquero, F. de Dios-Anton, V. Barroso, A. Rodriguez, D. W. Gray, M. Navarro, V. Kumar, A. Sherstnev, D. H. Drewry, J. R. Brown, J. M. Fiandor, J. Julio Martin, *Sci. Rep.* **2015**, *5*, 8771.
- [17] R. Brenk, A. Schipani, D. James, A. Krasowski, I. H. Gilbert, J. A. Frearson, P. G. Wyatt, *ChemMedChem* **2008**, *3*, 435–444.
- [18] H. van de Waterbeemd, G. Camenisch, G. Folkers, J. R. Chretien, O. A. Raevsky, *J. Drug Targeting* **1998**, *6*, 151–165.
- [19] T. T. Wager, R. Y. Chandrasekaran, X. Hou, M. D. Troutman, P. R. Verhoest, A. Villalobos, Y. Will, *ACS Chem. Neurosci.* **2010**, *1*, 420–434.
- [20] T. T. Wager, X. Hou, P. R. Verhoest, A. Villalobos, *ACS Chem. Neurosci.* **2010**, *1*, 435–449.
- [21] T. T. Wager, A. Villalobos, P. R. Verhoest, X. J. Hou, C. L. Shaffer, *Expert Opin. Drug Discovery* **2011**, *6*, 371–381.
- [22] M. P. Gleeson, *J. Med. Chem.* **2008**, *51*, 817–834.
- [23] P. Gleeson, G. Bravi, S. Modi, D. Lowe, *Bioorg. Med. Chem.* **2009**, *17*, 5906–5919.
- [24] M. Ishikawa, Y. Hashimoto, *J. Med. Chem.* **2011**, *54*, 1539–1554.
- [25] F. Lovering, J. Bikker, C. Humblet, *J. Med. Chem.* **2009**, *52*, 6752–6756.
- [26] M. De Rycker, S. O'Neill, D. Joshi, L. Campbell, D. W. Gray, A. H. Fairlamb, *PLoS Neglected Trop. Dis.* **2012**, *6*, e1932.
- [27] J. Witherington, V. Bordas, A. Gaiba, N. S. Garton, A. Naylor, A. D. Rawlings, B. P. Slingsby, D. G. Smith, A. K. Takle, R. W. Ward, *Bioorg. Med. Chem. Lett.* **2003**, *13*, 3055–3057.
- [28] M. O. Taha, Y. Bustanji, M. A. Al-Ghoussein, M. Mohammad, H. Zalloum, I. M. Al-Masri, N. Atallah, *J. Med. Chem.* **2008**, *51*, 2062–2077.
- [29] C. H. T. Chen, B. Eastman, A. Gosberg, S. N. Gradl, G. Hirst, S. D. Hopkins, K. T. T. Nguyen, R. Pracitto, P. E. Sprengeler, R. W. Steensma (SGX Pharmaceuticals Inc.), US Pat. No. US 20080261921 A1, **2008**.
- [30] M. Ohtsuka, N. Haginoya, M. Ichikawa, H. Matsunaga, H. Saito, Y. Shibata, T. Tsunemi (Daiichi Sankyo Co. Ltd.), US Pat. No. US 20110082138 A1, **2011**.

- [31] D. S. Mortensen, J. Sapienza, B. G. Lee, S. M. Perrin-Ninkovic, R. Harris, G. Shevlin, J. S. Parnes, B. Whitefield, M. Hickman, G. Khambatta, R. R. Bissonette, S. Peng, J. C. Gamez, J. Leisten, R. K. Narla, K. E. Fultz, S. Sankar, *Bioorg. Med. Chem. Lett.* **2013**, *23*, 1588–1591.
- [32] "Inhibition of Phosphorylation of Pras40, Gsk3-Beta or P70s6k1 as a Marker for Tor Kinase Inhibitory Activity", W. Xu, D. S. Mortensen, S. M. Xu, K. E. Fultz (Signal Pharmaceuticals LLC), Int. PCT Pub. No. WO 2014066125 A3, **2014**
- [33] G. Y. Leshner, E. R. Bacon, B. Singh, G.-H. Kuo (Sterling Drug Inc.) US Pat. No. US 5010086 A, **1991**.
- [34] K. W. Bair, T. Baumeister, A. J. Buckmelter, K. H. Clodfelter, P. Dragovich, F. Gosselin, B. Han, J. Lin, D. J. Reynolds, B. Roth, C. C. Smith, Z. Wang, P.-W. Yuen, X. Zheng (Forma Therapeutics Inc., Genentech Inc.), Int. PCT Pub. No. WO 2012031197 A1, **2012**.
- [35] S. Brand, L. A. Cleghorn, S. P. McElroy, D. A. Robinson, V. C. Smith, I. Halbyburton, J. R. Harrison, N. R. Norcross, D. Spinks, T. Bayliss, S. Norval, L. Stojanovski, L. S. Torrie, J. A. Frearson, R. Brenk, A. H. Fairlamb, M. A. Ferguson, K. D. Read, P. G. Wyatt, I. H. Gilbert, *J. Med. Chem.* **2012**, *55*, 140–152.
- [36] B. Rätz, M. Iten, Y. Grether-Bühler, R. Kaminsky, R. Brun, *Acta Trop.* **1997**, *68*, 139–147.

Received: July 10, 2015

Published online on September 18, 2015